Generator coordinate method calculations of one-nucleon removal reactions on ^{40}Ca

M. V. Ivanov, M. K. Gaidarov, and A. N. Antonov
Institute of Nuclear Research and Nuclear Energy, Bulgarian Academy of Sciences, Sofia 1784, Bulgaria

C. Giusti
Dipartimento di Fisica Nucleare e Teorica, Università di Pavia, Istituto Nazionale di Fisica Nucleare, Sezione di Pavia, Pavia, Italy
(Received 20 April 2000; revised manuscript received 12 January 2001; published 8 June 2001)

An approach to the generator coordinate method (GCM) using Skyrme-type effective forces and Woods-Saxon construction potential is applied to calculate the single-particle proton and neutron overlap functions in ^{40}Ca. The relationship between the bound-state overlap functions and the one-body density matrix has been used. These overlap functions are applied to calculate the cross sections of one-nucleon removal reactions such as $(e,e'p)$, (γ,p), and (p,d) on ^{40}Ca on the same theoretical footing. A consistent description of data for the different reactions is achieved. The shapes of the experimental cross sections for transitions to the $3/2^+$ ground state and the first $1/2^+$ excited state of the residual nuclei are well reproduced by the overlap functions obtained within the GCM. An additional spectroscopic factor accounting for correlations not included in the overlap function must be applied to the calculated results to reproduce the size of the experimental cross sections.

DOI: 10.1103/PhysRevC.64.014605 PACS number(s): 21.60.−n, 25.30.Dh, 25.20.−x, 25.40.Hs

I. INTRODUCTION

Experiments on nuclear reactions accompanied by one-nucleon removal from ^{40}Ca (e.g., Ref. [1–4]) have accumulated much spectroscopic information on its nucleon-hole spectral density function and, generally, on the single-particle aspects of nuclear structure. From the theoretical point of view two topics in the analyses of these processes are of significant interest and have been mainly studied: the reaction mechanism and the ground-state correlation effects. The latter can be successfully considered by using the unique relationship between the overlap functions (OF) related to bound states of the $(A-1)$-particle system and the one-body density matrix (ODM) of the A-particle system in its ground state [5]. This makes it possible to investigate the effects of the various types of nucleon-nucleon correlations included in the ODM on the bound-state proton and neutron overlap functions.

In our recent works [6,7] a consistent study of overlap functions and one-nucleon removal reactions on ^{16}O using different correlation methods has been carried out and comparison with the experimental data has been performed. In our previous calculations we used methods which account mainly for short-range and tensor nucleon-nucleon correlations. It is desirable, however, to take into consideration also correlations originating from the collective motion of the nucleons. This was partially done for the ^{16}O nucleus in Ref. [7]. In this respect, the various applications of the generator coordinate method to nuclear problems [8–10] have shown its efficiency as a potential source of information on nucleon-nucleon correlations in nuclei. The results on the one- and two-body density and momentum distributions, occupation probabilities, and natural orbitals obtained within the GCM using various construction potentials [10] have shown that the nucleon-nucleon correlations accounted for in this method are different from the short-range ones and are rather related to the collective motion of the nucleons. It was pointed out that these correlations are also important in calculations of other single-particle properties, such as one-body overlap functions, which are necessary in the calculations of cross sections of one-nucleon removal reactions.

It is known that, in general, when going from light to heavier systems the collectivity becomes stronger. Because of its undeformed closed-shell structure, the medium-heavy ^{40}Ca nucleus is one of the few nuclei for which microscopic calculations can be performed. For instance, only recently the Fermi hypernetted chain theory has been extended to describe the ground-state properties of ^{40}Ca [11]. Therefore, it is very attractive to probe its ''doubly magic'' character also in calculations of different types of one-nucleon removal reactions. As a first step differential cross sections for the ^{40}Ca(p,d) pickup reaction have been calculated in [12] with overlap functions obtained from the ODM in the Jastrow correlation method (JCM) [13]. Although only short-range correlations have been included in the OF, it was shown that the angular distributions obtained are in a qualitative agreement with the empirical (p,d) data for the transition to the ground state of the residual nucleus. These results have clearly pointed out the necessity of inclusion of another kind of *NN* correlations, namely the long-range correlations, corresponding to collective degrees of freedom. Better agreement with the experimental ^{16}O$(e,e'p)$ and ^{16}O(γ,p) data was achieved in Ref. [7], where it was concluded that the long-range correlations affect the spectroscopic factors causing an additional depletion of the quasihole states.

The main aim of the present work is to study the effects of the nucleon-nucleon correlations included in the generator coordinate method on the behavior of the bound-state proton and neutron overlap functions in ^{40}Ca and of the related one-nucleon removal reaction cross sections. We first calculate both proton and neutron single-particle overlap functions and spectroscopic factors on the basis of the corresponding proton (with included Coulomb interaction) and neutron one-body density matrices of the ^{40}Ca nucleus obtained with GCM using the relationship between the ODM's and the

0556-2813/2001/64(1)/014605(8)/$20.00

overlap functions. Second, these bound-state OF are used to calculate the cross sections of the ^{40}Ca$(e,e'p)$, ^{40}Ca(γ,p), and ^{40}Ca(p,d) reactions. Thus it becomes possible to investigate the role of the correlations related to collective nucleon motions and accounted for in the GCM on the overlap functions and one-nucleon removal cross sections in ^{40}Ca also in comparison with data.

In Sec. II we give the basic theoretical relationships necessary to obtain the one-body density matrix in GCM and the bound-state overlap functions by means of the asymptotic behavior of ODM. The results of the calculations of overlap functions and cross sections of $(e,e'p)$, (γ,p), and (p,d) reactions on ^{40}Ca are presented and discussed in Sec. III. Section IV contains the concluding remarks.

II. THE THEORETICAL SCHEME

A. The GCM ground-state one-body density matrix

We start from a standard GCM-type A-particle wave function Ψ when one real generator coordinate x is considered [14], i.e.,

$$\Psi(\{\mathbf{r}_i\}) = \int_0^\infty f(x)\Phi(\{\mathbf{r}_i\},x)dx, \quad i=1,\dots,A. \tag{1}$$

In Eq. (1) $\Phi(\{\mathbf{r}_i\},x)$ is the generating function, $f(x)$ is the generator or weight function and A is the mass number of the nucleus.

The application of the Ritz variational principle $\delta E=0$ leads to the Hill-Wheeler integral equation [14,15] for the weight function and the energy of the system

$$\int_0^\infty [\mathcal{H}(x,x') - EI(x,x')]f(x')dx' = 0, \tag{2}$$

where

$$\mathcal{H}(x,x') = \langle \Phi(\{\mathbf{r}_i\},x)|\hat{H}|\Phi(\{\mathbf{r}_i\},x')\rangle \tag{3}$$

and

$$I(x,x') = \langle \Phi(\{\mathbf{r}_i\},x)|\Phi(\{\mathbf{r}_i\},x')\rangle \tag{4}$$

are the energy and overlap kernels, respectively, and $\hat{H}$ is the Hamiltonian of the system. Solving the Hill-Wheeler equation (2) one can obtain the solutions $f_0,f_1,\dots,$ for the weight functions which correspond to the eigenvalues of the energy $E_0,E_1,\dots$.

The corresponding ground-state one-body density matrix is given by (see, e.g., Ref. [9])

$$\rho(\mathbf{r},\mathbf{r}') = \int\int f_0(x)f_0(x')I(x,x')\rho(x,x',\mathbf{r},\mathbf{r}')dxdx', \tag{5}$$

with

$$\rho(x,x',\mathbf{r},\mathbf{r}') = 4\sum_{\lambda,\mu=1}^{A/4} [N^{-1}(x,x')]_{\mu\lambda}\varphi_\lambda^*(\mathbf{r},x)\varphi_\mu(\mathbf{r}',x'), \tag{6}$$

where $\varphi_\lambda(\mathbf{r},x)$ are the single-particle wave functions corresponding to a given construction potential by means of which the generating single Slater determinant wave function $\Phi(\{\mathbf{r}_i\},x)$ is built. The matrix $N^{-1}_{\lambda\mu}(x,x')$ in Eq. (6) is the inverse matrix of

$$N_{\lambda\mu}(x,x') = \int \varphi_\lambda^*(\mathbf{r},x)\varphi_\mu(\mathbf{r},x')d\mathbf{r}. \tag{7}$$

As is known, the results of the GCM calculations depend on the type of the construction potential used to define the single-particle wave functions $\varphi_\lambda(\mathbf{r},x)$. In the present work we choose the Woods-Saxon (WS) potential as a construction potential with the diffuseness parameter as a generator coordinate. The GCM scheme, which has been already adopted in Ref. [7], gives a very good agreement with the data for the ^{16}O$(e,e'p)$ and ^{16}O(γ,p) reaction cross sections. In our present calculations the Skyrme-type effective force SkM* [16] is used, with parameters which give realistic binding energy of ^{40}Ca obtained from the Hill-Wheeler equation. The agreement of the calculated basic nuclear characteristics with their empirical values obtained in Ref. [10], proved once more the reliability of these effective forces, which are also used in the present study.

B. The overlap functions for the proton and neutron bound states

For a correct calculation of the cross section of nuclear reactions with one-neutron or one-proton removal from the target nucleus, the corresponding overlap functions for the neutron and proton bound states must be used in the reaction amplitudes. The construction of the ground-state ODM of ^{40}Ca from the generator coordinate method calculations makes it possible to apply the procedure for extracting single-particle overlap functions [5]. Here we would like to remind the reader that the single-particle overlap functions are defined by the overlap integrals between eigenstates of the A particle and the $(A-1)$-particle systems:

$$\phi_\alpha(\mathbf{r}) = \langle \Psi_\alpha^{(A-1)}|a(\mathbf{r})|\Psi^{(A)}\rangle, \tag{8}$$

where $a(\mathbf{r})$ is the annihilation operator for a nucleon with spatial coordinate $\mathbf{r}$ (spin and isospin operators are implied). In the mean-field approximation $\Psi^{(A)}$ and $\Psi_\alpha^{(A-1)}$ are single Slater determinants, and the overlap functions are identical with the mean-field single-particle wave functions, while in the presence of correlations both $\Psi^{(A)}$ and $\Psi_\alpha^{(A-1)}$ are complicated superpositions of Slater determinants. In general, the overlap functions (8) are not orthogonal. Their norm defines the spectroscopic factor

$$S_\alpha = \langle \phi_\alpha|\phi_\alpha\rangle. \tag{9}$$

The normalized overlap function associated with the state α then reads

$$\tilde{\phi}_\alpha(\mathbf{r}) = S_\alpha^{-1/2}\phi_\alpha(\mathbf{r}). \tag{10}$$

The one-body density matrix [e.g., Eq. (5)] can be expressed in terms of the overlap functions in the form

$$\rho(\mathbf{r},\mathbf{r}')=\sum_{\alpha} \phi_{\alpha}^{*}(\mathbf{r})\phi_{\alpha}(\mathbf{r}')=\sum_{\alpha} S_{\alpha}\tilde{\phi}_{\alpha}^{*}(\mathbf{r})\tilde{\phi}_{\alpha}(\mathbf{r}'). \tag{11}$$

It is known (e.g., Ref. [17]) that the overlap function associated with the bound state ($\alpha\equiv nlj$) of the $(A-1)$- or $(A+1)$-nucleon system is an eigenstate of a single-particle Schrödinger equation in which the mass operator plays the role of a potential. Due to its finite range, the asymptotic behavior of the radial part of the neutron overlap functions for the bound states of the $(A-1)$ system is given by [5,18]

$$\phi_{nlj}(r)\rightarrow C_{nlj}\exp(-k_{nlj}r)/r, \tag{12}$$

where k_{nlj} is related to the neutron separation energy

$$k_{nlj}=\frac{\sqrt{2m\epsilon_{nlj}}}{\hbar}, \quad \epsilon_{nlj}=E_{nlj}^{(A-1)}-E_{0}^{A}. \tag{13}$$

For proton bound states, due to an additional long-range part originating from the Coulomb interaction, the asymptotic behavior of the radial part of the corresponding proton overlap functions reads

$$\phi_{nlj}(r)\rightarrow C_{nlj}\exp[-k_{nlj}r-\eta\ln(2k_{nlj}r)]/r, \tag{14}$$

where η is the Coulomb (or Sommerfeld) parameter and k_{nlj} in Eq. (13) contains in this case the mass of the proton and the proton separation energy.

Taking into account Eqs. (11) and (12), the lowest ($n=n_0$) neutron bound-state lj-overlap function is determined by the asymptotic behavior of the associated partial radial contribution of the one-body density matrix $\rho_{lj}(r,r')$ ($r'=a\rightarrow\infty$) as

$$\phi_{n_0lj}(r)=\frac{\rho_{lj}(r,a)}{C_{n_0lj}\exp(-k_{n_0lj}a)/a}, \tag{15}$$

where the constants C_{n_0lj} and k_{n_0lj} are completely determined by $\rho_{lj}(a,a)$. In this way the separation energy ϵ_{n_0lj} and the spectroscopic factor S_{n_0lj} can be determined as well. Similar expression for the lowest proton bound-state overlap function can be obtained having in mind its proper asymptotic behavior (14).

The applicability of this theoretical procedure has been demonstrated in Refs. [6,7,13]. In particular, it has been shown [7] that the substantial realistic inclusion of short-range as well as tensor correlations in the ODM of ^{16}O constructed within the Green function method [19] and, as a consequence, in the extracted overlap functions, leads to a fair and consistent description of the experimental cross sections of the ^{16}O$(e,e'p)$ and ^{16}O(γ,p) reactions. The importance of collective long-range correlations on the additional spectroscopic factors extracted in comparison with data has been also pointed out in Ref. [7].

In this work we use as a basis the GCM results for the correlated states of ^{40}Ca obtained in Ref. [10], where correlations due to collective nucleon motion are properly taken into account. The procedure to calculate the overlap functions from the one-body density matrix outlined above is performed numerically for ^{40}Ca within the GCM. In this respect we would like to note that an important condition of this procedure is the exponential asymptotics of the overlap functions at $r'\rightarrow\infty$ [see Eqs. (12) and (14)], which is related to the correct asymptotics of $\rho_{lj}(r,r')$ at $r'\rightarrow\infty$. This condition is fulfilled in our GCM approach by using realistic single-particle Woods-Saxon wave functions in the generating single Slater determinant wave function $\Phi(\{\mathbf{r}_i\},x)$ in Eq. (1). The exponential decay of the partial radial ODM is with a decay constant k_{nlj} related to the separation energy [Eq. (13)]. The question about the correct asymptotic behavior of the extracted overlap functions will also be discussed in Sec. III.

III. RESULTS AND DISCUSSION

In the present paper the GCM numerical calculations have been performed using Woods-Saxon construction potential with diffuseness parameter as a generator coordinate. The values of the radius and the depth of the construction potential have been fixed. Following Ref. [20], the value of the depth used for both neutron and proton cases has been taken to be 50 MeV, while the corresponding values of the potential radius are 1.30 fm for the neutron and 1.24 fm for the proton case, respectively. The effective SkM* interaction [16] is used, with parameter set values ($t_0=-2645, t_1=410, t_2=-135, t_3=15595, \sigma=1/6$), which give the realistic binding energy of ^{40}Ca obtained from the Hill-Wheeler equation (2). A discretization procedure is performed in order to solve this integral equation using a set of regular mesh points with steps as well as ranges of values of the generator coordinate which lead to the convergence of the results, i.e., the latter do not change after decreasing the step size or increasing the range of the generator coordinate value. The range of variation of the diffuseness parameter turns out to be within the interval 0.49–0.9072 fm. The ground-state energy and the excitation energy of the first monopole 0^+ state of ^{40}Ca derived from the procedure (340.07 and 20.4 MeV) are close to the corresponding experimental values (342.06 and 20.0 MeV [21], respectively). Likewise, in Ref. [10] the same GCM scheme gives a value for the excitation energy of the 0^+ breathing state in ^{16}O which is in a good agreement with the result obtained in Ref. [22].

The one-body density matrix (5) constructed within the GCM approach has been applied to calculate overlap functions related to the quasihole states in the ^{40}Ca nucleus. In our method the extracted overlap functions for a given orbital momentum l are the same for the different $j=l\pm1/2$. Hereafter the overlap functions for the neutron and proton $1d$ and $2s$ states will be of particular interest: transitions to the $3/2^+$ ground state and the first $1/2^+$ excited state of the corresponding residual nuclei observed in ^{40}Ca$(e,e'p)$, ^{40}Ca(γ,p), and ^{40}Ca(p,d) reactions will be considered. The squared overlap functions $|r\phi(r)|^2$ for the neutron and pro-

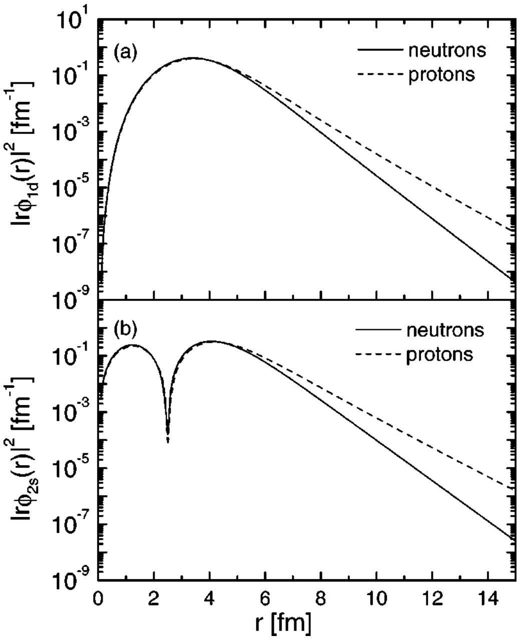

FIG. 1. $|r\phi(r)|^2$ for the neutron and proton $1d$ (a) and $2s$ (b) quasihole states in ^{40}Ca obtained with GCM. The normalization is $\int\phi^2(r)r^2dr=S$.

ton $1d$ and $2s$ quasihole states are illustrated in Fig. 1. They have the correct asymptotic behavior related to the exponential decrease of the ODM in its asymptotic region, being different for protons and neutrons. The latter is in accordance with the experimental proton and neutron separation energies. As is known, the one-neutron separation energy for ^{40}Ca is almost twice larger than the one-proton one and, therefore, the asymptotic tail of the GCM density matrix is dominated by the contribution from the proton overlap between the ^{40}Ca and ^{39}K ground-state wave functions, where the role of the Coulomb interaction is important.

The comparison of $|r\phi(r)|^2$ calculated with the GCM overlap functions and with the shell-model Woods-Saxon wave functions for the neutron bound states is given in Fig. 2. Small differences between the two functions can be seen for both $1d$ and $2s$ states. The same is valid also for the $1s$

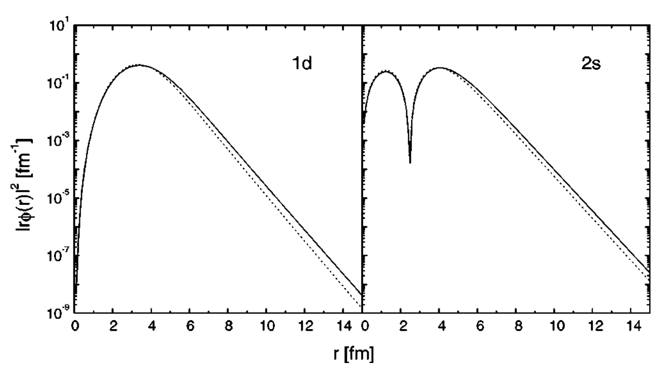

FIG. 2. $|r\phi(r)|^2$ for the neutron $1d$ and $2s$ quasihole states in ^{40}Ca obtained with GCM overlap function (solid line) and Woods-Saxon single-particle wave function $|r\varphi(r)|^2$ (dashed line). All curves are normalized to unity.

TABLE I. Neutron (ϵ_n) and proton (ϵ_p) separation energies (in MeV) calculated on the basis of the one-body density matrix for ^{40}Ca within the GCM. Comparison is made with the Hartree-Fock (HF) [23] single-particle energies, JCM results [13], and with the experimental data (exp.) [23]. The HF and exp. values are given for the $d_{3/2}$ state.

	ϵ_n				ϵ_p		
nl	GCM	HF	JCM	exp.	GCM	HF	exp.
$1d$	15.84	17.52	24.75	15.64	8.69	10.33	8.33
$2s$	14.15	19.51	13.07	18.19	7.39	12.42	10.94

and $1p$ quasihole states, not presented in the figure. This result justifies the approximation of using shell-model orbitals instead of overlap functions in calculating the nucleon knockout cross section for these nuclear states. Nevertheless, as has been pointed out in previous works [6,7], the calculated cross sections of one-nucleon removal reactions are very sensitive to the differences in the corresponding overlap functions.

The values of the neutron and proton separation energies derived from the procedure mentioned above are listed in Table I. It can be seen that the separation energies obtained within the GCM are very close to the experimental values for the $1d$ state of ^{40}Ca and are anyhow better than the JCM result for ϵ_n in the $2s$ state. In addition, we present the separation energy values obtained within the mean-field approximation (the Hartree-Fock method [23]). We should note that the differences between the latter and those from both correlation methods are dependent on whether the nucleons are in a valence orbital or not. Here we would like to note also that the use of Woods-Saxon wave functions (instead of, e.g., harmonic-oscillator wave functions as in the JCM calculation), which have the proper exponential-type decay, leads to a correct asymptotic behavior of the extracted overlap functions with satisfactory separation energies of the quasihole states.

The values of the spectroscopic factors deduced from the numerical procedure turn out to be very close to unity. This is not surprising, because tensor and short-range nucleon-nucleon correlations are not included in the GCM. As is known, these correlations are responsible for the bulk part of the depletion of the occupied states [6]. The values of the spectroscopic factors derived from the Jastrow correlation method [13], where short-range correlations are included, are 0.892 for the $1d$ state and 0.956 for the $2s$ state, respectively.

The reduced cross sections for the ^{40}Ca$(e,e'p)$ reaction as a function of the missing momentum p_m, i.e., the magnitude of the recoil momentum of the residual nucleus, for the transitions to the $3/2^+$ ground state and the first $1/2^+$ excited state (at excitation energy $E_x=2.522$ MeV) of ^{39}K are displayed in Figs. 3 and 4, respectively. Calculations have been done with the code DWEEPY [24], which is based on a nonrelativistic distorted wave impulse approximation (DWIA) description of the nucleon knockout process and includes final-state interactions and Coulomb distortion of the elec-

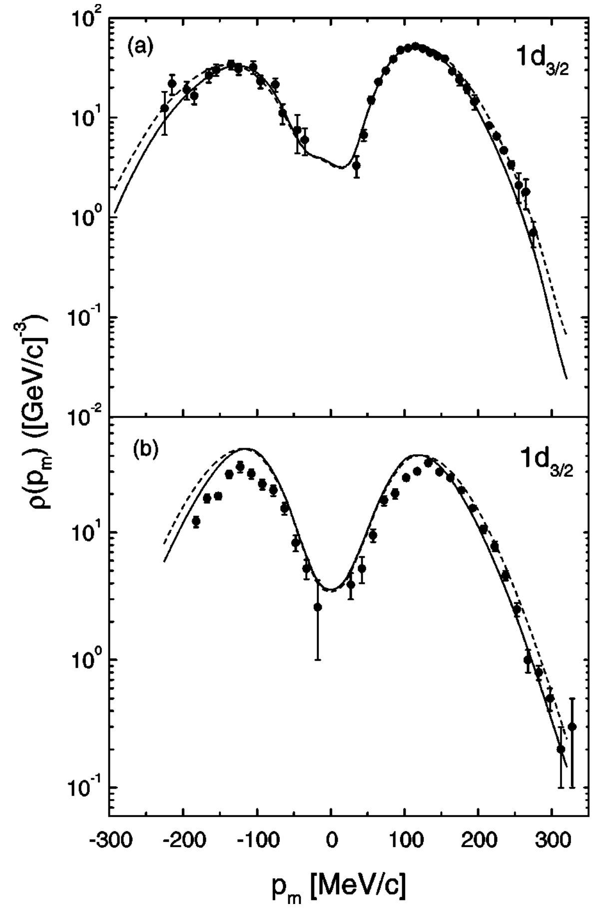

FIG. 3. Reduced cross section of the ^{40}Ca$(e,e'p)$ reaction as a function of the missing momentum p_m for the transition to the $3/2^+$ ground state of ^{39}K in parallel (a) and perpendicular (b) kinematics. The incident electron energy is 460 MeV in case (a), 483.2 MeV in case (b) and the outgoing proton energy is 100 MeV. The optical potential is taken from Ref. [30]. The overlap function is derived from the ODM of GCM (solid line). The dashed line is calculated with the WS wave function. The experimental data (full circles) are taken from Ref. [2]. The theoretical results have been multiplied by the reduction factors given in the text.

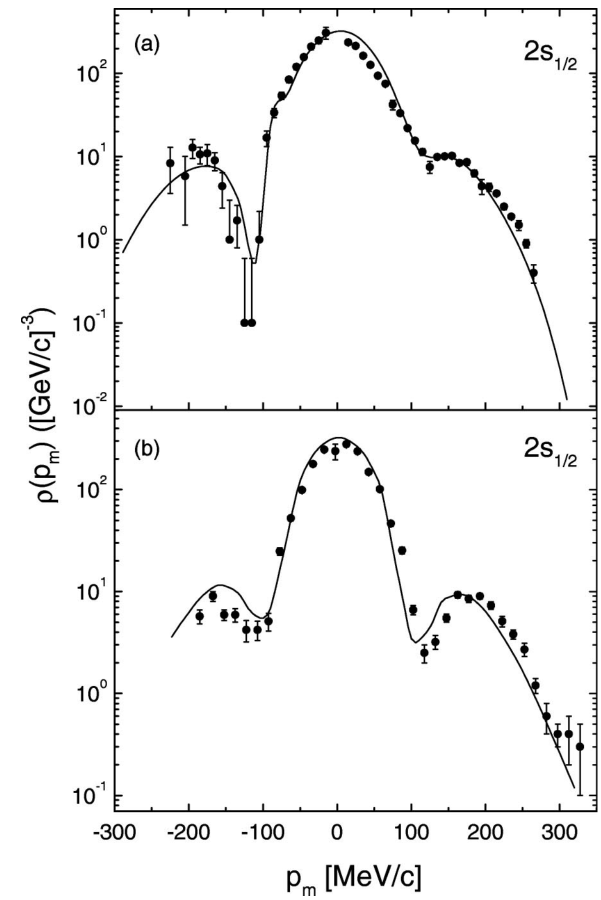

FIG. 4. The same as in Fig. 3 for the transition to the first $1/2^+$ excited state at 2.522 MeV of ^{39}K. The theoretical results have been multiplied by the reduction factor 0.50.

tron waves [25]. In the figures the results obtained with the overlap functions generated by the GCM are compared with the data from Ref. [2] in parallel and perpendicular kinematics. In parallel kinematics the momentum of the outgoing proton is fixed and is taken parallel or antiparallel to the momentum transfer. Different values of the missing momentum are then obtained by varying the electron scattering angle. In perpendicular kinematics the outgoing proton energy and the momentum transfer are kept constant and different values of the missing momentum are obtained by varying the angle of the outgoing proton.

A fair agreement with the shape of the experimental cross section is achieved for both transitions and kinematics with the overlap functions emerging from the ODM calculated within the GCM, which includes realistic correlations corresponding to single-particle and collective motion modes. The OF's already include the spectroscopic factors. In order to reproduce the size of the experimental cross section, an additional reduction factor has been applied to the theoretical results. As in our previous analysis of the ^{16}O$(e,e'p)$ reaction [7], this factor can be considered as a further spectroscopic factor, reflecting the correlations not included in the OF which correspondingly cause depletion of the quasihole states. The same reduction factor has been applied to the cross sections calculated with the OF for both parallel and perpendicular kinematics, namely, 0.55 for the $3/2^+$ ground state in Fig. 3 and 0.50 for the $1/2^+$ excited state in Fig. 4. Small variations around these values do not change significantly the comparison with the data. However, for the ground-state transition in perpendicular kinematics a reduction factor about 20% lower would give a better agreement with data. A different spectroscopic factor for this transition in the two kinematics is found also in the data analysis of Ref. [2], where in perpendicular kinematics the spectroscopic factor is 25% lower than the one determined in parallel kinematics. This discrepancy is related in Ref. [2] to the basic ingredients of the theory: the optical potential, the bound-state wave function, the electron distortion and the influence of meson-exchange currents (MEC). Our total spectroscopic factors (the norm of OF's multiplied by the additional reduction factor mentioned above) with the GCM, 0.54 for $3/2^+$ and 0.49 for $1/2^+$, are comparable with the ''experimental'' ones, 0.65 and 0.52, determined under parallel kinematical

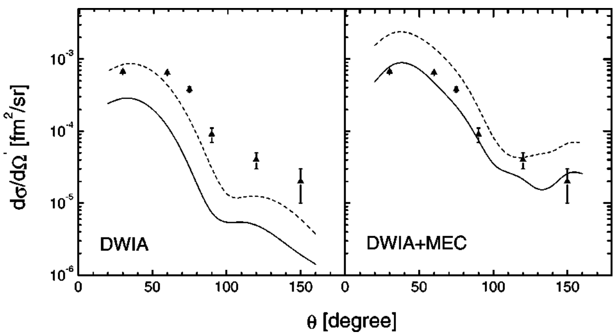

FIG. 5. Angular distribution of the ^{40}Ca(γ,p) reaction for the transition to the $3/2^{+}$ ground state of ^{39}K at $E_{\gamma}=60$ MeV. The optical potential is taken from Ref. [30]. The separate contributions given by the one-body current (DWIA) and the final result given by the sum of the one-body and the two-body seagull current (DWIA +MEC) are shown. Line convention is as in Fig. 3. The experimental data (triangles) are taken from Ref. [4]. The theoretical results have been multiplied by the reduction factors given in the text, consistent with the analysis of ($e,e'p$) data.

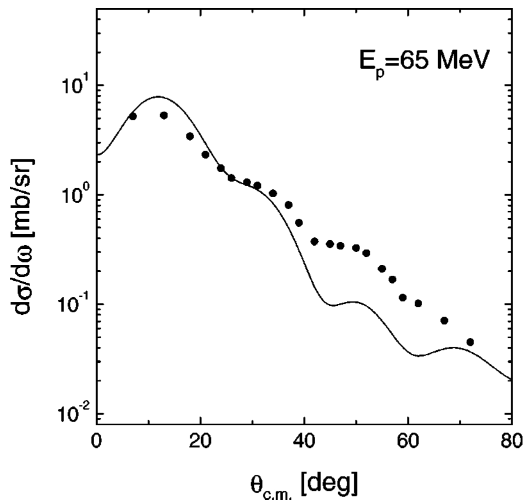

FIG. 6. Differential cross section for the ^{40}Ca(p,d) reaction at incident proton energy $E_{p}=65$ MeV for the transition to the $3/2^{+}$ ground state in ^{39}Ca. The neutron overlap function is derived from the ODM of GCM (solid line). The proton and deuteron optical potentials are taken from Refs. [31] and [32], respectively. The experimental data [1] are given by the full circles. The theoretical results have been multiplied by the reduction factor 0.55.

conditions in the analysis of Ref. [2], where the calculations are performed within the same DWIA framework and with the same optical potential, but where phenomenological single-particle wave functions are used with some parameters adjusted to the data. We emphasize that in the present analysis the overlap functions theoretically calculated on the basis of the ODM of ^{40}Ca within the GCM do not contain free parameters. Our spectroscopic factors are also in reasonable agreement with those extracted from the fully relativistic theoretical analysis of the ^{40}Ca($e,e'p$) reaction in Ref. [26], where, however, only a part of the ($e,e'p$) data from Ref. [2] is considered, while somewhat larger spectroscopic factors (around 0.7–0.8) are obtained in the relativistic analyses of Refs. [27,28].

In Fig. 3 for the ^{40}Ca($e,e'p$)^{39}K$_{\text{g.s.}}$ reaction we present also the results obtained with the phenomenological Woods-Saxon wave function. The WS wave function is also able to give a good description of the data with a reduction factor of 0.6625, somewhat larger than the one applied to the reduced cross section computed with GCM overlap function. Also with the WS wave function a reduction factor lower by about 20% would give a better description of the data in perpendicular kinematics.

Figure 5 shows the angular distribution of the ^{40}Ca(γ,p)^{39}K$_{\text{g.s.}}$ reaction at $E_{\gamma}=60$ MeV. In the figure the results given by the sum of the one-body and of the two-body seagull currents are compared with the contribution given by the one-body current, which roughly corresponds to the DWIA treatment based on the direct knockout (DKO) mechanism. Both contributions of DKO and MEC are consistently evaluated in the theoretical framework of Ref. [29]. The results obtained with the OF from GCM for the ground state transition and with the phenomenological WS wave function are compared in the figure. In order to check the consistency in the description of different one-proton removal reactions, the calculated cross sections have been multiplied by the same reduction factors obtained from the analysis of ($e,e'p$) data, i.e., 0.55 with GCM and 0.6625 with WS. The differences between the two curves are considerable and larger than in the ($e,e'p$) reaction. This result might have been expected, since it is well known that (γ,p) results are extremely sensitive to the theoretical ingredients adopted in the calculation, in particular for the bound states.

The GCM calculation lies well below the data in DWIA, but a reasonable agreement with the size and the shape of the experimental cross section is obtained when MEC are added. Thus, the important role played by MEC [7,29] is confirmed here also for the ^{40}Ca(γ,p) reaction. The WS calculations are larger than the ones with the GCM. This result can be understood also from Fig. 3, where at the high values of the missing momentum, that are explored in the (γ,p) reaction, the ($e,e'p$) reduced cross sections calculated with WS wave function are larger than the ones obtained with the OF from the GCM. Thus, in DWIA the WS result is closer to the data, in particular for the lowest angles, but when MEC are added it overshoots the experimental cross section.

Therefore, although both calculations with the GCM and WS wave functions are able to give a good description of the ^{40}Ca($e,e'p$) data for the transition to the $3/2^{+}$ ground state of ^{39}K, the (γ,p) results presented in Fig. 5 for the same transition show that the GCM overlap function leads to a better and more consistent description of data for the ($e,e'p$) and (γ,p) reactions. This result suggests proper accounting for the nucleon correlation effects in the framework of the GCM.

In Fig. 6 the differential cross section of the ^{40}Ca(p,d) reaction for the transition to the $3/2^{+}$ ground state in ^{39}Ca, calculated at incident proton energy $E_{p}=65$ MeV with the neutron GCM overlap function, is given and compared with the experimental data [1]. It has been obtained using the distorted wave Born approximation (DWBA) with zero-range approximation for the p-n interaction inside the deuteron. It is well known that the cross section of the (p,d) reaction is more sensitive to the reaction mechanism adopted than to the choice of the bound-state wave function. In this respect quasifree nucleon knockout reactions are more suitable for our investigation. Nevertheless, within the DWBA for such a pickup process as the (p,d) reaction, it can be seen that the shape of the angular distribution is well reproduced by the GCM. Applying the total spectroscopic factor of 0.54 for $3/2^+$ state to the calculated cross section, a reasonable agreement with the size of the experimental cross section is achieved. The role of the additional depletion or reduction of the spectroscopic factors due to correlations not included in the OF has been already seen on the examples of the previous reactions considered. Although some differences between the calculated and experimental angular distributions exist, we would like to emphasize that, in principle, overlap functions extracted from realistic one-body density matrices have to be used as a tool for an accurate description of one-nucleon removal reactions.

IV. CONCLUSIONS

In summary, we have calculated single-particle overlap functions and the spectroscopic factors corresponding to low-lying (quasihole) $(A-1)$-nucleon states on the base of the one-body density matrix of ^{40}Ca by considering its asymptotic (large r) region and using the generator coordinate method. These calculations have been performed within an approach in which a Woods-Saxon construction potential and a Skyrme-type effective force are used. A consistent analysis of the cross sections of one-nucleon removal reactions on ^{40}Ca by means of the same overlap functions is given. In contrast to standard DWIA analyses, where phenomenological single-particle wave functions were used with some parameters fitted to the data, in this paper the results have been obtained with theoretically calculated overlap functions which do not include free parameters. The differences between the GCM overlap functions and the shell model WS wave functions for both hole and particle states are analyzed as a test for the role of correlations inherent to our approach.

We have found that the calculated cross sections are generally in good agreement with the experimental data. The quality of the agreement, however, is sensitive to details of the overlap functions. The important role of the additional reduction spectroscopic factor applied to the present calculations is pointed out. The fact that the reduction factor is consistent in different nucleon removal reactions and also that this result is obtained both for ^{40}Ca in the present work and for ^{16}O in Ref. [7] gives a more profound theoretical meaning to this parameter. It can be interpreted as the spectroscopic factor accounting for correlations not included in the generator coordinate method. The values of the total spectroscopic factors obtained in the present analysis are in reasonable agreement with those given by previous theoretical investigations.

Apart from the short-range and tensor correlations studied in previous papers [6,7], in this work we looked into the role of correlations caused by the collective nucleon motion. Exploring the GCM, a consistent picture for all three $(e,e'p)$, (γ,p), and (p,d) reactions on ^{40}Ca was achieved on the same theoretical ground. The results indicate that the effects of NN correlations taken into account within our approach and which are of long-range type are of significant importance for the correct analysis of the processes considered.

Finally, we would like to emphasize that the theoretical method to calculate the cross sections of one-nucleon removal reactions by means of single-particle overlap functions for the bound states presented in this paper is, in principle, valid for all kind of nuclei. The particular GCM scheme employed in our work is applicable, however, only to nuclei with equal numbers of protons and neutrons but to both closed and nonclosed shell nuclei. Calculations of similar reactions on open s-d shell nuclei are in progress.

ACKNOWLEDGMENTS

We acknowledge the financial support given by the Bulgarian National Science Foundation under Contracts No. Φ–809 and Φ–905.

[1] P. G. Roos, S. M. Smith, V. K. C. Cheng, G. Tibell, A. A. Cowley, and R. A. A. Riddle, Nucl. Phys. **A255**, 187 (1975).
[2] J. Kramer, Ph.D. thesis, Universiteit van Amsterdam, 1990.
[3] L. Lapikás, Nucl. Phys. **A553**, 297c (1993).
[4] C. Van den Abeele, D. Ryckbosch, J. Ryckebusch, J. Dias, L. Van Hoorebeke, R. Van de Vyver, J.-O. Adler, B.-E. Andersson, L. Isaksson, H. Ruijter, and B. Schröder, Phys. Lett. B **296**, 302 (1992).
[5] D. Van Neck, M. Waroquier, and K. Heyde, Phys. Lett. B **314**, 255 (1993).
[6] M. K. Gaidarov, K. A. Pavlova, S. S. Dimitrova, M. V. Stoitsov, A. N. Antonov, D. Van Neck, and H. Müther, Phys. Rev. C **60**, 024312 (1999).
[7] M. K. Gaidarov, K. A. Pavlova, A. N. Antonov, M. V. Stoitsov, S. S. Dimitrova, M. V. Ivanov, and C. Giusti, Phys. Rev. C **61**, 014306 (2000).
[8] A. N. Antonov, Chr. V. Christov, and I. Zh. Petkov, Nuovo Cimento A **91**, 119 (1986); A. N. Antonov, I. S. Bonev, Chr. V. Christov, and I. Zh. Petkov, *ibid.* **100**, 779 (1988); A. N. Antonov, I. S. Bonev, and I. Zh. Petkov, Bulg. J. Phys. **18**, 169 (1991); A. N. Antonov, I. S. Bonev, Chr. V. Christov, and I. Zh. Petkov, Nuovo Cimento A **103**, 1287 (1990).
[9] A. N. Antonov, P. E. Hodgson, and I. Zh. Petkov, *Nucleon Correlations in Nuclei* (Springer-Verlag, Berlin, 1993); *Nucleon Momentum and Density Distributions in Nuclei* (Clarendon, Oxford, 1988).
[10] M. V. Ivanov, A. N. Antonov, and M. K. Gaidarov, Int. J. Mod. Phys. E **9**, 339 (2000).
[11] F. Arias de Saavedra, G. Co', A. Fabrocini, and S. Fantoni, Nucl. Phys. **A605**, 359 (1996); F. Arias de Saavedra, G. Co',

and M. M. Renis, Phys. Rev. C **55**, 673 (1997); A. Fabrocini, F. Arias de Saavedra, and G. Co', *ibid.* **61**, 044302 (2000).
[12] S. S. Dimitrova, M. K. Gaidarov, A. N. Antonov, M. V. Stoitsov, P. E. Hodgson, V. K. Lukyanov, E. V. Zemlyanaya, and G. Z. Krumova, J. Phys. G **23**, 1685 (1997).
[13] M. V. Stoitsov, S. S. Dimitrova, and A. N. Antonov, Phys. Rev. C **53**, 1254 (1996).
[14] J. J. Griffin and J. A. Wheeler, Phys. Rev. **108**, 311 (1957).
[15] D. L. Hill and J. A. Wheeler, Phys. Rev. **89**, 1102 (1953).
[16] J. Bartel, P. Quentin, M. Brack, C. Guet, and H. B. Håkansson, Nucl. Phys. **A386**, 79 (1982).
[17] C. Mahaux and R. Sartor, Adv. Nucl. Phys. **20**, 1 (1991).
[18] J. M. Bang, F. A. Gareev, W. T. Pinkston, and J. S. Vaagen, Phys. Rep. **125**, 253 (1985).
[19] A. Polls, H. Müther, and W. H. Dickhoff, *Proceedings of Conference on Perspectives in Nuclear Physics at Intermediate Energies*, Trieste, 1995, edited by S. Boffi, C. Ciofi degli Atti, and M. M. Giannini (World Scientific, Singapore, 1996), p. 308.
[20] H. P. Blok and J. H. Heisenberg, in *Computational Nuclear Physics 1, Nuclear Structure*, edited by K. Langanke, J. A. Maruhn, and S. E. Koonin (Springer-Verlag, Berlin, 1991), p. 190.
[21] N. A. Voinova-Eliseeva and I. A. Mitropolsky, Report No. LINP 1104, 1985 (unpublished).
[22] D. M. Brink and G. F. Nash, Nucl. Phys. **40**, 608 (1963).
[23] C. Mahaux and R. Sartor, Nucl. Phys. **A528**, 253 (1991).
[24] C. Giusti and F. D. Pacati, Nucl. Phys. **A473**, 717 (1987); **A485**, 461 (1988).
[25] S. Boffi, C. Giusti, F. D. Pacati, and M. Radici, *Electromagnetic Response of Atomic Nuclei*, *Oxford Studies in Nuclear Physics* (Clarendon Press, Oxford, 1996).
[26] J. M. Udias, P. Sarriguren, E. Moya de Guerrra, E. Garrido, and J. A. Caballero, Phys. Rev. C **48**, 2731 (1993).
[27] Y. Jin, D. S. Onley, and L. E. Wright, Phys. Rev. C **45**, 1311 (1992).
[28] J. L. Johansson, H. S. Sherif, and G. M. Lotz, Nucl. Phys. **A605**, 517 (1996).
[29] G. Benenti, C. Giusti, and F. D. Pacati, Nucl. Phys. **A574**, 716 (1994).
[30] P. Schwandt, H. O. Meyer, W. W. Jacobs, A. D. Bacher, S. E. Vigdor, M. D. Kaitchuck, and T. R. Donoghue, Phys. Rev. C **26**, 55 (1982).
[31] C. B. Fulmer *et al.*, Phys. Rev. **181**, 1565 (1969).
[32] F. D. Becchetti and G. W. Greenlees, Phys. Rev. **182**, 1190 (1969).